Modification to Adaptive Model Reduction for Regulation of Distributed Parameter Systems with Fast Transients

Davood Babaei Pourkargar and Antonios Armaou
Dept. of Chemical Engineering, The Pennsylvania State University, University Park, PA 16802

DOI 10.1002/aic.14207
Published online September 6, 2013 in Wiley Online Library (wileyonlinelibrary.com)

We focus on output feedback control of distributed processes whose infinite dimensional representation in appropriate Hilbert subspaces can be decomposed to finite dimensional slow and infinite dimensional fast subsystems. The controller synthesis issue is addressed using a refined adaptive proper orthogonal decomposition (APOD) approach to recursively construct accurate low dimensional reduced order models (ROMs) based on which we subsequently construct and couple almost globally valid dynamic observers with robust controllers. The novelty lies in modifying the data ensemble revision approach within APOD to enlarge the ROM region of attraction. The proposed control approach is successfully used to regulate the Kuramoto-Sivashinsky equation at a desired steady state profile in the absence and presence of uncertainty when the unforced process exhibits nonlinear behavior with fast transients. The original and the modified APOD approaches are compared in different conditions and the advantages of the modified approach are presented. © 2013 American Institute of Chemical Engineers *AIChE J*, 59: 4595–4611, 2013
Keywords: process control, nonlinear systems, distributed parameter systems, adaptive model reduction, APOD

Introduction

In recent years, the interest in control of nonlinear distributed parameter systems (DPSs) has significantly increased due to the need to synthesize controllers for complex transport-reaction processes that are characterized by the coupling of chemical reaction with significant convection, diffusion, and dispersion phenomena. Such processes as exemplified by catalytic reactions, polymerization processes, plasma etching, and semiconductor manufacturing, exhibit spatial variations that need to be explicitly accounted by the controller.[1–5]

An important observation is that the long term behavior of the above chemical processes can be captured by a finite number of degrees of freedom, thus, the infinite dimensional partial differential equation (PDE) description can be approximated by reduced order models (ROMs) in the form of ordinary differential equations (ODEs).[6] A widely used method to compute the ROM, is the method of weighted residuals. The prerequisite basis functions can be obtained either analytically or using statistical methods such as proper orthogonal decomposition (POD).[7] POD generates optimal orthogonal empirical eigenfunctions that capture the energy of a data set to describe the data trends.[8] It has been used extensively in model reduction, sensor placement, optimization, and control of distributed processes.[3,9–13] Another approach to obtain basis functions is based on balanced realizations, which has been studied extensively to obtain stability and error analysis results, especially for linear systems.[14–16]

Correspondence concerning this article should be addressed to A. Armaou at armaou@engr.psu.edu.

The POD approach assumes *a priori* availability of a sufficiently large ensemble of PDE solution data which excites the most prevalent spatial modes. Such an ensemble is necessary to characterize the behavior of the system dynamics and compute empirical eigenfunctions in this method. However, in practice, it is difficult to generate such an ensemble so that all possible dominant spatial modes are appreciably contained within the corresponding snapshots. The resulting eigenfunctions, therefore, are representative of the corresponding ensemble only. During closed-loop simulation, situations may arise when the existing eigenfunctions fail to accurately represent the dynamics of the PDE system.

A solution is to initially compute the eigenfunctions using the available ensemble of snapshots, and then to recompute the eigenfunctions as needed when more information from the system becomes available.[17] However, this would require the solution of the eigenvalue-eigenvector problem every time, which may become computationally expensive, and hence, unsuitable for online computations as the process evolves. To reduce the computational load and to circumvent the limitation of sufficiently large ensemble of profile data, the recursive computation of eigenfunctions, known as adaptive POD (APOD), could be used as additional data from the process becomes available to design tailored feedback control structures.[17–19] The requirements on continuous measurement sensors were then reduced using APOD-based dynamic observers.[20] The performance of the controller structure hinges on the frequency of the sampling which must be of the same order as the frequency of the appearance of new trends.

In this manuscript, output feedback controllers are designed for fast evolving DPSs based on continuous point measurements available from limited number of sensors and

infrequent distributed snapshots. The developed methodology for robust output feedback control is based on the successful integration of dynamic observers with static controllers. A refined ensembling approach is used in APOD to recursively update the eigenfunctions as the closed-loop process evolves through different regions of the state space based on maximizing retained information that is received from the infrequent distributed sensor measurements. The proposed controller is illustrated on the Kuramoto-Sivashinsky equation (KSE) with and without uncertainty in the presence of highly nonlinear dynamics and chaotic behavior, where they are called to stabilize the system at an open-loop unstable system steady state. The original and the modified ensemble construction approaches for APOD are compared in different conditions and the robustness of modified APOD with respect to uncertainty, number of snapshots and number of continuous point sensors and their locations is illustrated.

Mathematical Preliminaries

We focus on the output feedback regulation problem of spatially distributed processes described by the following state space description of highly dissipative PDEs

$$\begin{aligned} \frac{\partial x}{\partial t} &= \mathbf{A}(z)x + \mathbf{F}\left(z, x, \frac{\partial x}{\partial z}, ..., \frac{\partial^{n_0} x}{\partial z^{n_0}}\right) + b(z)u \\ y_m &= \int_\Omega s_m(z)x dz \\ y_r &= s_r(z,t)x \end{aligned} \tag{1}$$

subject to the following boundary conditions

$$q\left(x, \frac{dx}{d\eta}, ..., \frac{d^{n_0-1}x}{d\eta^{n_0-1}}\right) = 0 \text{ on } \partial\Omega \tag{2}$$

and initial condition

$$x(z,0) = x_0(z) \tag{3}$$

In the above PDE system, t is the time, $z \in \Omega \subset \mathbb{R}^3$ is the spatial coordinate, Ω is the domain of the process and $\partial\Omega$ is its boundary. $x(z,t) \in \mathbb{R}^n$ denotes the vector of state variables. $u \in \mathbb{R}^l$ denotes the vector of manipulated inputs. $\mathbf{A}(z)$ is a linear spatial differential operator of order n_0 (where n_0 is an even number). $\mathbf{F}$ is a bounded purely nonlinear and possibly differential function of order up to n_0. $b(z) \in \mathbb{R}^{n \times l}$ is a smooth matrix function of z of the form $[b_1(z)b_2(z)...b_l(z)]$, where $b_i(z)$ describes how the ith control action $u_i(t)$ is distributed in the spatial domain Ω, for example, point actuation could be defined using Dirac delta. In (2), $q(\cdot)$ is a sufficiently smooth nonlinear vector function, $\frac{dx}{d\eta}|_{\partial\Omega}$ denotes the derivative in the direction perpendicular to the boundary and $x_0(z)$ is a smooth vector function of z. The availability of two types of measurement sensors is assumed: periodic snapshot measurements, $y_r(z) \in \mathbb{R}^n$, to measure spatial profiles and continuous measurements, $y_m \in \mathbb{R}^r$, where r is the number of continuous sensors. $s_r(z,t)$ and $s_m(z)$ are the sensor shape functions corresponding to y_r and y_m, respectively. In the remainder of the article, we present our results for $x \in \mathbb{R}$. It is conceptually straightforward to extend the results to $x \in \mathbb{R}^n$, usually by treating each state individually.[21]

The control objective is to stabilize the process of (1)–(3) at a desired spatial profile, $x_d(z)$. Without loss of generality, we assume the spatially uniform steady state $x_d(z)=0$ as the desired profile. We also assume that long term and dominant dynamic behavior of the system of (1)–(3) can be captured by a finite number of degrees of freedom. This implies that, in principle, the long term dynamics of state x of the mentioned system can be accurately described by a finite number of appropriately chosen basis functions.

The PDE system of (1) can be represented as an infinite dimensional system in an approximately chosen Hilbert space, $\mathcal{H}(\Omega, \mathbb{R})$, where space derivatives are defined. The inner product and norm in the space of square integrable functions, $L_2[\Omega]$, is defined as

$$(\vartheta_1, \vartheta_2) = \int_\Omega \vartheta_1^T(z)\vartheta_2(z)dz \qquad \text{and } ||\vartheta_1||_2 = (\vartheta_1, \vartheta_1)^{1/2}$$

where ϑ^T denotes the transpose. The state $a \in \mathcal{H}(\Omega, \mathbb{R})$ is defined as

$$a(t) = x(z,t) \tag{4}$$

where

$$\mathbb{H} = \left\{ a \in \mathcal{H}(\Omega, \mathbb{R}); q\left(a, \frac{da}{d\eta}, ..., \frac{d^{n_0-1}a}{d\eta^{n_0-1}}\right) = 0 \text{ on } \partial\Omega \right\} \tag{5}$$

and the linear differential operator and purely nonlinear function, respectively

$$\begin{aligned} \mathcal{A}a &= \mathbf{A}(z)x, \\ F(a) &= \mathbf{F}\left(z, x, \frac{dx}{dz}, ..., \frac{d^{n_0}x}{dz^{n_0}}\right) \end{aligned} \tag{6}$$

and the input and measured output operators as $\mathcal{B}u = b(z)u, S_m a = \int_\Omega s_m(z)x dz, S_r a = s_r(z,t)x$. The PDE system of (1) can then be expressed in the following form

$$\begin{aligned} \dot{a} &= \mathcal{A}a + F(a) + \mathcal{B}u, a(0) = a_0 \\ y_m &= S_m a, \\ y_r &= S_r a. \end{aligned} \tag{7}$$

F is a nonlinear smooth vector function that satisfies $F(0)=0$ and the Lipschitz condition locally

$$||F(a_1) - F(a_2)||_2 \leq K_l ||a_1 - a_2||_2 \tag{8}$$

where K_l indicates the upper bound gain in the Lipschitz inequality.

The eigenvalue problem for the operator $\mathcal{A}$ can be defined as follows

$$\mathcal{A}\phi_i = \lambda_i \phi_i, \; i = 1, ..., \infty \tag{9}$$

where $\lambda_i \in \mathbb{R}$ and $\phi_i \in \mathbb{H}$ denote the eigenvalues and the corresponding eigenfunctions, respectively. Note that the eigenspectrum of $\mathcal{A}$, $\{\lambda_1, \lambda_2, ...\}$, indicates a subspace partitioning of $\mathbb{H}$ as it can be partitioned into a finite dimensional set of s slow eigenvalues, $\{\lambda_1, \lambda_2, ..., \lambda_s\}$, and a stable infinite dimensional complement set of the remaining fast eigenvalues $\{\lambda_{s+1}, \lambda_{s+2}, ...\}$, where the eigenvalues are ordered in terms of value as follows

$$\lambda_1 > \lambda_2 > ... > \lambda_s \gg \lambda_{s+1} > ...$$

There is a large separation between the slow and fast eigenvalues of $\mathcal{A}$.[6]

Finite dimensional approximation

Considering the infinite dimensional representation of the system in an appropriate functional space, the state modes

can be partitioned into a finite number of slow and possibly unstable modes and an infinite number of stable and fast modes and there is a time scale separation between the dynamic behavior of the two subsystems. Such an approach will lead to accurate finite dimensional ODE models for processes that exhibit strong diffusive phenomena (and can thus be described by highly dissipative PDE systems); this is due to the fact that their dominant dynamic behavior can be captured by a finite number of dominant spatial profiles.

The Hilbert space, $\mathbb{H}$, can be partitioned into two subspaces, one that includes finite number of slow and possibly unstable modes, $\mathbb{H}_s$, and a complement subspace that includes infinite number of fast and stable modes, $\mathbb{H}_f$. By defining the following orthogonal projection operators, the state of system (7) can be described as

$$a = a_s + a_f = \mathcal{P}_H a + \mathcal{Q}_H a \tag{10}$$

where $a_s = \mathcal{P}_H a \in \mathbb{H}_s$, $a_f = \mathcal{Q}_H a \in \mathbb{H}_f$, $\mathcal{P}_H : \mathbb{H} \to \mathbb{H}_s$, $\mathcal{Q}_H : \mathbb{H} \to \mathbb{H}_f$, and $\mathbb{H} = \mathbb{H}_s \oplus \mathbb{H}_s$. Using (10), the system (7) can be expressed in the following form

$$\begin{aligned} \dot{a}_s &= A_s(a_s, a_f) + F_s(a_s, a_f) + B_s u \\ \dot{a}_f &= A_f(a_s, a_f) + F_f(a_s, a_f) + B_f u \\ a_s(0) &= P_H a_0 \\ a_f(0) &= Q_H a_0 \\ y_m &= S_m a_s + S_m a_f \\ y_r &= S_r a_s + S_r a_f \end{aligned} \tag{11}$$

where $A_s = \mathcal{P}_H \mathcal{A}(a_s + a_f)$, $A_f = \mathcal{Q}_H \mathcal{A}(a_s + a_f)$, $F_s = \mathcal{P}_H F$, $F_f = \mathcal{Q}_H F$, $B_s = \mathcal{P}_H \mathcal{B}$, $B_f = \mathcal{Q}_H \mathcal{B}$

The infinite dimensional fast and stable subsystem can be neglected using singular perturbation arguments (section 4.5 in Ref. 6). Thus the long term dynamic behavior of the fast system subspace can be described by $a_f \equiv 0$ and the following approximation is obtained from the system of (11)

$$\begin{aligned} \dot{a}_s &= A_s(a_s, 0) + F_s(a_s, 0) + B_s u \\ y_m &= S_m a_s \\ y_r &= S_r a_s \end{aligned} \tag{12}$$

Considering $\mathbb{H} = \text{span}\{\phi_1, \phi_2, \ldots\}$, we can derive a vector form of the system of (7). $\mathbb{H}$ can be partitioned into two subspaces, one that includes first s eigenfunctions, $\mathbb{H}_s = \text{span}\{\phi_1, \phi_2, \ldots, \phi_s\}$, and a complement subspace that includes the rest of eigenfunctions, $\mathbb{H}_f = \text{span}\{\phi_{s+1}, \phi_{s+2}, \ldots\}$.

It should be noted that a vector representation of the system of (7) can be obtained by applying weighted residual methods to (1) and keeping the first s ODEs and neglecting the fast and stable subsystem.[6] The type of weighted residual method could be determined by the weighting functions in the above equation. The method of weighted residuals reduces to Galerkin's method when the weighting functions and the basis functions are the same. Obtained from the basis functions, the ROM can be summarized as

$$\begin{aligned} \dot{a} &= \mathscr{A} a + \mathscr{F}(a) + \mathscr{B} u \\ y_m &= \mathscr{C} a \end{aligned} \tag{13}$$

where $\mathscr{A}$, $\mathscr{B}$, and $\mathscr{C}$ are constant matrices and $\mathscr{F}$ is a nonlinear smooth vector function of the modes. Equation 13 is a vector representation of the system of (12), that is, a_s in (12) is a vector function in slow and stable Hilbert subspace, $\mathbb{H}_s$, but a in (13) is a vector in real space, $\mathbb{R}^s$.

We assume that F satisfies the Lipschitz condition as follows

$$||\mathscr{F}(a_1) - \mathscr{F}(a_2)||_2 \leq K_l ||a_1 - a_2||_2$$

where K_l indicates the upper bound gain in the Lipschitz inequality.

Problem Formulation

The issue with the analysis of the previous section is that the basis functions, ϕ, can rarely be derived analytically. To circumvent this issue, we use statistical methods to obtain them when they are unavailable.

Initially, snapshots of the state profile of the system during process evolution are collected to construct an ensemble of snapshots similar to the other data-driven model reduction and control methodologies. In previous methods, a large ensemble ensemble of solutions must be constructed by gathering state profile snapshots for different values of input variable, $u(t)$, and different initial conditions[22,23] while the recursive update of empirical eigenfunctions in APOD disposes of this requirement.

Empirical eigenfunctions computation

The off-line solution data of the process are used to construct the basis functions that are necessary to derive the ROMs of (13). Let the collection of K snapshots be called the ensemble represented in a vector function form, $v(z) = [x(z, t_1), \ldots, x(z, t_K)]^T$. Each snapshot is the spatial profiles of the system states at a particular time instant obtained either experimentally by initially gathering open-loop process evolution data before activating the controller or from previously obtained process history data, or by performing off-line numerical simulations of the PDE system. The off-line part of APOD is used to compute an orthogonal set of basis functions for the representation of the ensemble which are called empirical eigenfunctions of the process. It also provides a measure of the relative contribution of each function to the total energy of the ensemble (energy represents the information content of the ensemble) and it is an efficient way for computing basis functions that capture the dominant patterns of the ensemble.

Let C_K denote the covariance matrix of the ensemble obtained from K snapshots that is defined as follows

$$C_K := \int_\Omega v v^T dz \tag{14}$$

The solution of the computationally expensive optimization problem to identify the best basis functions that describe the snapshot ensemble is circumvented through the solution of an eigenvalue-eigenvector problem of the covariance matrix of the snapshot ensemble, which may also be computationally demanding depending on the ensemble size. The key features of the algorithm and a detailed analysis have been presented in, and they closely resemble standard POD.[17]

The eigenspace of the covariance matrix can be partitioned into two subspaces; the dominant one containing the eigenfunctions which capture at least ε percent of energy in the ensemble (denoted as $\mathbb{P}$) and the orthogonal complement to $\mathbb{P}$ containing the rest of the modes (denoted as $\mathbb{Q}$). Such

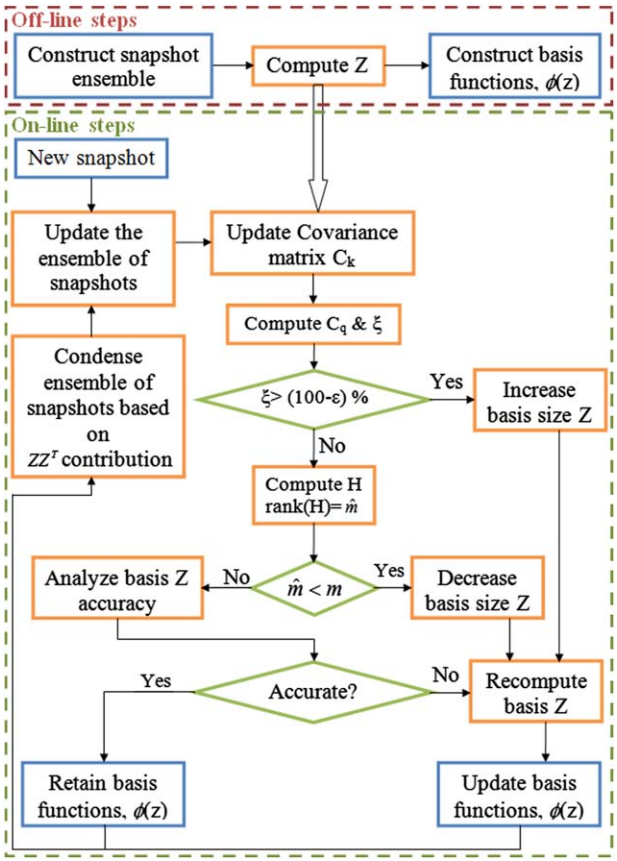

Figure 1. Flow chart of adaptive model reduction methodology.

Blue boxes denote algorithm I/Os and green decision steps. [Color figure can be viewed in the online issue, which is available at wileyonlinelibrary.com.]

a partition is possible because the ensemble is snapshots of a dissipative system evolution and the dominant dynamics of highly dissipative PDEs are finite dimensional.[24]

Solving the eigenvalue problem for C_K we obtain μ_i and ω_i that denoted the ith eigenvalue and eigenvector where the eigenvalues are ordered in terms of value as follows

$$\mu_1 > \mu_2 > \ldots > \mu_K$$

It is assumed that m eigenvectors out of K possible eigenvectors of C_K have the corresponding eigenvalues such that

$$\sum_{i=1}^{m} \mu_i / \sum_{i=1}^{K} \mu_i \geq \frac{\varepsilon}{100}$$

that is, m eigenfunctions of C_K capture ε percent of energy in the ensemble.

An orthonormal basis for the subspace $\mathbb{P}$ can be obtained as:

$$Z=[\omega_1, \omega_2, \ldots, \omega_m], Z \in \mathbb{R}^{K \times m} \tag{15}$$

Note that the underlying assumption of all POD and balanced realization methods is that eigenfunctions computed by these eigenvectors also capture the dominant dynamics of the PDE system of (1–3) locally.

We can compute the eigenfunctions, ψ, as a linear combination of the snapshots

$$\psi_i(z)=\omega_i^T v, i=1, \ldots, m \tag{16}$$

During system evolution, the online component of APOD allows updating the empirical eigenfunctions on-line once new measurements from the process become available.

The orthogonal projection operators P_A and Q_A onto subspaces $\mathbb{P}$ and $\mathbb{Q}$ respectively, can be computed[17,18] as follows

$$P_A=ZZ^T, Q_A=I-ZZ^T \tag{17}$$

where I denotes the identity matrix of dimension K.

The details of the methodology are presented in Refs. 17–19.

The performance of the controller structure hinges on the local validity of the ROM. To have a valid ROM, it is necessary to update the ensemble, used for computation of the basis functions, based on the new snapshots arrived from the system during the process evolution. The following two approaches are considered to generate the new ensemble of snapshots that is used to compute the covariance matrix in the next time step when the new snapshot arrives.

The Newest Snapshots Approach. In this approach, the newest snapshots are considered in the ensemble of snapshots. In each time step during closed-loop process evolution, the oldest snapshot of the system, v_1, will be replaced by the new snapshot obtained by the periodic snapshot measurements, y_r. Thus, in each time step the ensemble only includes the most recent snapshots. In this article, APOD using this data ensembling is called the "original APOD."

In the original APOD, the ensemble of the snapshots that is used to update the basis functions only possesses the most recent snapshots. The procedure could possibly lead to loss of previously important profiles as the process evolves away from them and they are replaced by profiles that contain new information. If the process revisits a previously accessed

state space region, APOD has to recapture the new trends as they reaffirm themselves leading to a lag in the ROM revision that captures the new trends.

The Most Important Snapshots Approach. The modification analyzes the contribution of snapshots in $\mathbb{P}$ by normalized dominant eigenvectors and search for the one which had the minimum 2-norm per row and eliminates the corresponding snapshot in the ensemble. To formulate the procedure, consider the contribution column vectors of $D=\{d_j\}$ and standardization column vector of $S=\{s_j\}$, respectively, as follows

$$d_j=\left(P_A P_A^T\right)_{jj} \tag{18}$$

where $(\cdot)_{jj}$ indicates the diagonal element of $(\cdot)$ and

$$s_j=||C_{K,j}||_2 \tag{19}$$

where $||\cdot||_2$ indicates the 2-norm of vector $(\cdot)$ and $C_{K,j}$ means the jth row of the covariance matrix and $j=1,\ldots,K$.

The normalized snapshot contribution column vector, $N=\{n_j\}$, is defined based on (20).

$$n_j=\frac{d_j}{s_j}, j=1,\ldots,K \tag{20}$$

We eliminate the snapshot that corresponds to the element in the normalized snapshot contribution vector that has the lowest value.

The ensemble condensation by most dependent snapshot elimination can be performed before or after addition of the new snapshot in C_K. If the elimination takes place after augmenting the new snapshot to the ensemble, there is a possibility to eliminate the new data at each revisions. To circumvent this problem, the least important snapshots are eliminated before adding the new one, in order to have the most recent snapshot and also the most important ones. This is called the "modified APOD."

A move to consider the most important snapshots instead of newest ones thus leads to faster and more infrequent revision of the ROM when regions of the state space are previously revisited. Control design based on this ROM leads to larger region of accuracy which is important when dealing with model uncertainty and fast evolving processes. Also the dynamic observer that is constructed based on the basis functions from this modified APOD is more insensitive to the available number of point measurements and their locations; in most cases, we can use only one sensor without being concerned about sensor placement using robust nature of modified APOD. The other advantage of the refined approach is using smaller ensemble of snapshots during the closed-loop process evolution that leads reduction in load of covariance matrix computation and saving run-time. A flow chart illustrating the revised APOD approach is presented in Figure 1.

Consider the local subspace of the slow and unstable modes, $\mathbb{H}_s=\text{span}\{\phi_1,\phi_2,\ldots,\phi_s\}$ and subspace $\mathbb{P}$ defined as $\mathbb{P}=\text{span}\{\psi_1,\psi_2,\ldots,\psi_m\}$, where $\{\phi\}$ is the set of unavailable basis functions of the system and $\{\psi\}$ is the set of basis functions computed based on APOD. We assumed that $\mathbb{H}_s\subseteq\mathbb{P}$, locally, due to the excitation of the higher modes during the closed-loop process evolution providing richer behavior than the slow subsystem would.

Remark 1. *The modified data ensembling approach increases the computation time of APOD by 10%. However, it leads to more robust ROMs that require revisions more infrequently, as will be illustrated in the Application section.*

Remark 2. *In the proposed approach for model reduction, the snapshots used are obtained during closed-loop system evolution as opposed to most other POD-based reduction approaches that are based on open-loop snapshots. Thus, these snapshots and the resulting ROM account for the impact of controller functional form on the process. It is important to note this intimate relation between APOD and the controller.*

Dynamic observer design

We assume that the snapshots of the process become available only periodically and the point measurements from a restricted number of sensors are continuously available which is quite common in industrial processes. In Refs. 17, 18, static output observers based on the continuous point measurements were designed to estimate the modes of (13) that are required for controller design. The number of sensors had to be supernumerary to the number of modes to successfully estimate the modes of (13) using the linear static observers. This implies that numerous measurement sensors are required, otherwise the static observer gives erroneous estimates. Also, the static observer existence depends on the location and shape of the measurement sensors. To overcome these issues, we used a dynamic observer that conceptually needs only one point measurement to predict the dynamic behavior of the modes as long as the process is observable at that position.[25]

The theory on linear dynamic observer design was developed by Luenberger in Ref. 26 and offered a complete and comprehensive analysis. Nonlinear dynamic observer design is much more complicated and has received considerable attention in the last 30 years.[27–29]

We can define the observation error based on the Hilbert subspace representation of the system of (1) as follows

$$\varepsilon(z,t)=\hat{x}(z,t)-x(z,t) \tag{21}$$

where $\hat{x}$ and x are the observer and system states of (1)–(3), respectively.

By neglecting the fast and stable part of the process system dynamic behavior and using separation of variables, we can define the observer state

$$\hat{x}(z,t)=\psi^T(z)\hat{a}(t) \tag{22}$$

and the original state

$$x(z,t)=\phi^T(z)a(t) \tag{23}$$

where $\psi=[\psi_1\psi_2\ldots\psi_m]^T$, $\phi=[\phi_1\phi_2\ldots\phi_s]^T$; m is the number of empirical eigenfunctions of the slow subsystems that are computed using APOD and s is the number of unavailable eigenfunctions of the slow subsystem.

The dimension of the system slow modes, a and $\hat{a}$ in Eqs. 22 and 23, respectively, is not necessarily the same because the number of identified slow subsystem basis functions $\{\phi\}$ and $\{\psi\}$ may be different; so the observation error can not be defined directly by the simple subtraction, $\hat{a}-a$.

From (23) we could define a mapping between two subspaces, $\mathbb{H}_s$ and $\mathbb{P}$ as follows

$$x=\phi^T a=\psi^T\mathcal{M}a=\psi^T\tilde{a} \tag{24}$$

where $\tilde{a}=\mathcal{M}a$, $\mathcal{M}:\mathbb{H}_s\mapsto\mathbb{P}$ and

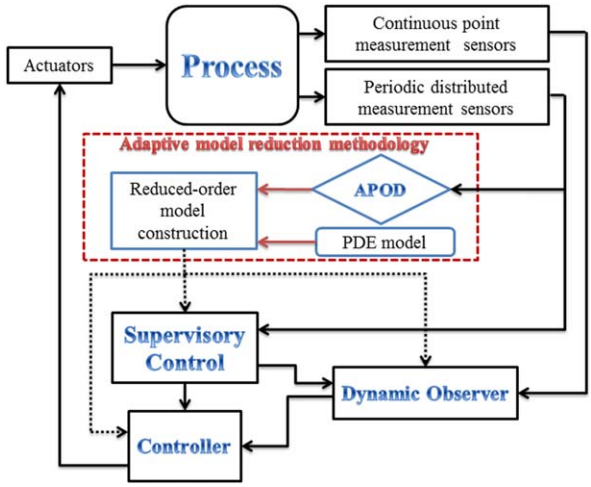

Figure 2. Process operation block diagram under proposed controller structure.

[Color figure can be viewed in the online issue, which is available at wileyonlinelibrary.com.]

$$\mathcal{M}=\int_{\Omega}\psi\phi^{T}dz \tag{25}$$

Using the above transformation, the system eigenmode dynamics in (13) can be expressed using the basis functions of subspace $\mathbb{P}$ in the following form

$$\begin{aligned}\dot{\tilde{a}}&=A\tilde{a}+f(\tilde{a})+Bu\\ y_m&=C\tilde{a}\end{aligned} \tag{26}$$

while the dynamic observer based on (26) will have the following structure

$$\dot{\hat{a}}=A\hat{a}+f(\hat{a})+Bu+L(C\hat{a}-y_m) \tag{27}$$

where $\hat{a}$ is the vector of estimated modes, A and B are constant matrices between ROM revisions. L is the observer gain, C is the output matrix, and f is locally Lipschitz continuous. Also the observation error could be defined within subspace $\mathbb{P}$ as follows

$$\varepsilon=\hat{x}-x\simeq\psi^{T}e \tag{28}$$

where $e=\hat{a}-\tilde{a}$.

Assuming observability and controllability of the system (26), we used pole placement approaches to compute the observer gain, L, that stabilizes the system of (27) in the Lyapunov sense. To implement the pole placement technique the observer error is defined as $e=\hat{a}-\mathcal{M}a=\hat{a}-\tilde{a}$. The observer error dynamics can be defined using (26) and (27) as follows

$$\dot{e}=(A+LC)e+[f(\hat{a})-f(\hat{a}-e)] \tag{29}$$

If the following Lyapunov function is considered

$$V=\frac{\zeta_{o}}{2}e^{T}e+\frac{\zeta_{c}}{2}\tilde{a}^{T}\tilde{a} \tag{30}$$

where V_o and V_c are the observer Lyapunov function (OLF) and the control Lyapunov function (CLF), respectively, and ζ_o and ζ_c are appropriately chosen positive numbers, the time derivative of Lyapunov function will be $\dot{V}=\zeta_{o}e^{T}\dot{e}+\zeta_{c}\tilde{a}^{T}\dot{\tilde{a}}$

Considering the control objective, $\tilde{a}\rightarrow 0$ and the CLF $V_c=\frac{\zeta}{2}\tilde{a}^{T}\tilde{a}$, we assume a controller can be designed that forces the time derivative of the CLF, $\tilde{a}^{T}\dot{\tilde{a}}$ to be negative. Then we need only establish that

$$\dot{V}=\zeta_{o}e^{T}\dot{e}=\zeta_{o}(e^{T}(A+LC)e+e^{T}[f(\hat{a})-f(\hat{a}-e)])<0 \tag{31}$$

If f satisfies the Lipschitz condition as follows

$$||f(\hat{a})-f(\hat{a}-e)||_{2}\leq K_{l}||e||_{2} \tag{32}$$

where K_l indicates the upper bound gain in the Lipschitz inequality, then

$$\begin{aligned}e^{T}[f(\hat{a})-f(\hat{a}-e)]&\leq||e^{T}||_{2}||f(\hat{a})-f(\hat{a}-e)||_{2}\\ &\leq||e^{T}||_{2}K_{l}||e||_{2}=K_{l}||e||_{2}^{2}=K_{l}e^{T}e\end{aligned} \tag{33}$$

Inequality (31) can be stated as follows using (33)

$$\begin{aligned}e^{T}(A+LC)e+e^{T}(K_{l}I)e<0&\Rightarrow e^{T}(A+LC+K_{l}I)e<0\\ &\Rightarrow A+LC+K_{l}I<0\end{aligned} \tag{34}$$

The above inequality problem can be solved using pole placement for $A+K_lI+LC=A_o+LC$. The closed-loop observer error poles are the eigenvalues of $A_c=A_o+LC$, which can be arbitrarily assigned by proper selection of the observer gain matrix, L. The observer gain matrix, L, is chosen such that

$$|sI-(A_{o}+LC)|=p_{\mathrm{des}}(s) \tag{35}$$

where I is the identity matrix and p_{des} is the characteristic polynomial of desired poles.

An extension to this approach can be made based on linear quadratic regulation. Equation 35 can be expressed as

$$|sI-(A_{o}+LC)|=|(sI-(A_{o}+LC))^{T}|=|sI-(A_{o}^{T}+C^{T}L^{T})| \tag{36}$$

where A_o^T and C^T are the dual system matrices in (37) and L^T is the state feedback gain matrix in state feedback control problem of the dual system

$$\begin{aligned}\dot{\tilde{e}}&=A_{o}^{T}\tilde{e}+C^{T}\tilde{u}\\ \tilde{u}&=L^{T}\tilde{e}\end{aligned} \tag{37}$$

Linear quadratic state feedback regulator theory[30] is used to solve the dual control problem and to compute the gain matrix. In (37), the state feedback law minimizes the following quadratic objective function

$$J(\tilde{u})=\int_{0}^{\infty}\left(\tilde{e}^{T}Q(\zeta_{o})\tilde{e}+\tilde{u}^{T}R\tilde{u}+2\tilde{e}^{T}N\tilde{u}\right)dt \tag{38}$$

subject to the system dynamics in (37). $Q(\zeta_o)$, R and N are positive definite matrices. The optimal gain matrix L^T can be calculated for the mentioned optimization problem as follows

$$L^{T}=-\left(R^{-1}\left(B^{T}S+N^{T}\right)\right)^{T}\Rightarrow L=-\left(N+S^{T}B\right)R^{-T} \tag{39}$$

where S is the solution of the associated Riccati equation

$$A_{o}S+SA_{o}^{T}-\left(SC^{T}+N\right)R^{-1}\left(CS+N^{T}\right)+Q=0 \tag{40}$$

Further details of these dynamic observer designs and linear matrix inequality based designs are presented in Ref. 20.

Proposition 1. *For the system of (26), the observation error under the observer of (27) with observer feedback gain, L, from (39) is locally stable in the Lyapunov sense.*

See Appendix A for proof.

Remark 3. *Note that $\mathcal{M}:\mathbb{H}_{s}\mapsto\mathbb{P}$ is an injective map because subspace $\mathbb{P}$ contains $\mathbb{H}_s$ and a part of subspace $\mathbb{H}_f$.*

By construction, when $\tilde{a}_1=\tilde{a}_2$, $\forall \tilde{a}_1,\tilde{a}_2 \in \mathbb{P}$ implies $a_1=a_2$, $\forall a_1,a_2 \in \mathbb{H}_s$, which is necessary for observer and controller design purposes. Due to this construction, a reverse map, $\mathcal{M}^{\perp}:\mathbb{P}\mapsto\mathbb{H}_s$, can be in principle defined such that $\mathcal{M}^{\perp}\mathcal{M}:\mathbb{H}_s\mapsto\mathbb{H}_s$ is a bijective map.

Output feedback controller design

In this section, we focus on the controller structure design using Lyapunov's direct method to achieve the stabilization objective the system of (26) in the origin between ROM revisions.

Proposition 2. *Assuming separation principle for the system of (26), the following static output feedback control law*[6,31] *can asymptotically stabilize the system of (26).*

$$u(t)=-k(\tilde{a},c_o)(L_BV_c) \tag{41}$$

where

$$k(\tilde{a},c_o)=\begin{pmatrix} c_o+\dfrac{L_FV_c+\sqrt{(L_FV_c)^2+(|||(L_BV_c)|||)^4}}{(|||(L_BV_c)|||)^2}, L_BV_c\neq 0 \\ c_o, \quad L_BV_c=0 \end{pmatrix}$$

$V_c=\frac{\zeta_c}{2}\tilde{a}^T\tilde{a}$ *is the CLF,* $L_BV_c=[L_{B_1}V_c\ldots L_{B_l}V_c]^T$ *is a column vector,* $L_FV_c=\frac{\partial V_c}{\partial \tilde{a}}F$ *and* $L_BV_c=\frac{\partial V_c}{\partial \tilde{a}}B$ *denote Lie derivatives.*

See Appendix B for proof.

Remark 4. *The positive parameter c_o allows a certain degree of flexibility in shaping the dynamic behavior of the closed-loop system. For example, a large value of c_o will force $\dot{V}_c$ to be more negative and therefore generate a faster transient response. Note that a positive value of c_o is not necessary for stabilization.*

Remark 5. *When implementing the controller of (41) in closed-loop process simulations, the numerical integrations could result in chattering-like behavior for the control input near origin. This problem is circumvented by adding a sufficiently small positive number η_c to $(L_{\mathcal{G}_i}V_c)^2$ in the denominator of (41). The addition of this parameter obviously leads to some offset in the closed-loop response. However, this offset can be made arbitrarily small by choosing a sufficiently small value for η_c. A tradeoff thus exists between the smoothness of the control action (corresponds to large η_c) and the smaller offset in the closed-loop response (corresponds to using small value for η_c).*

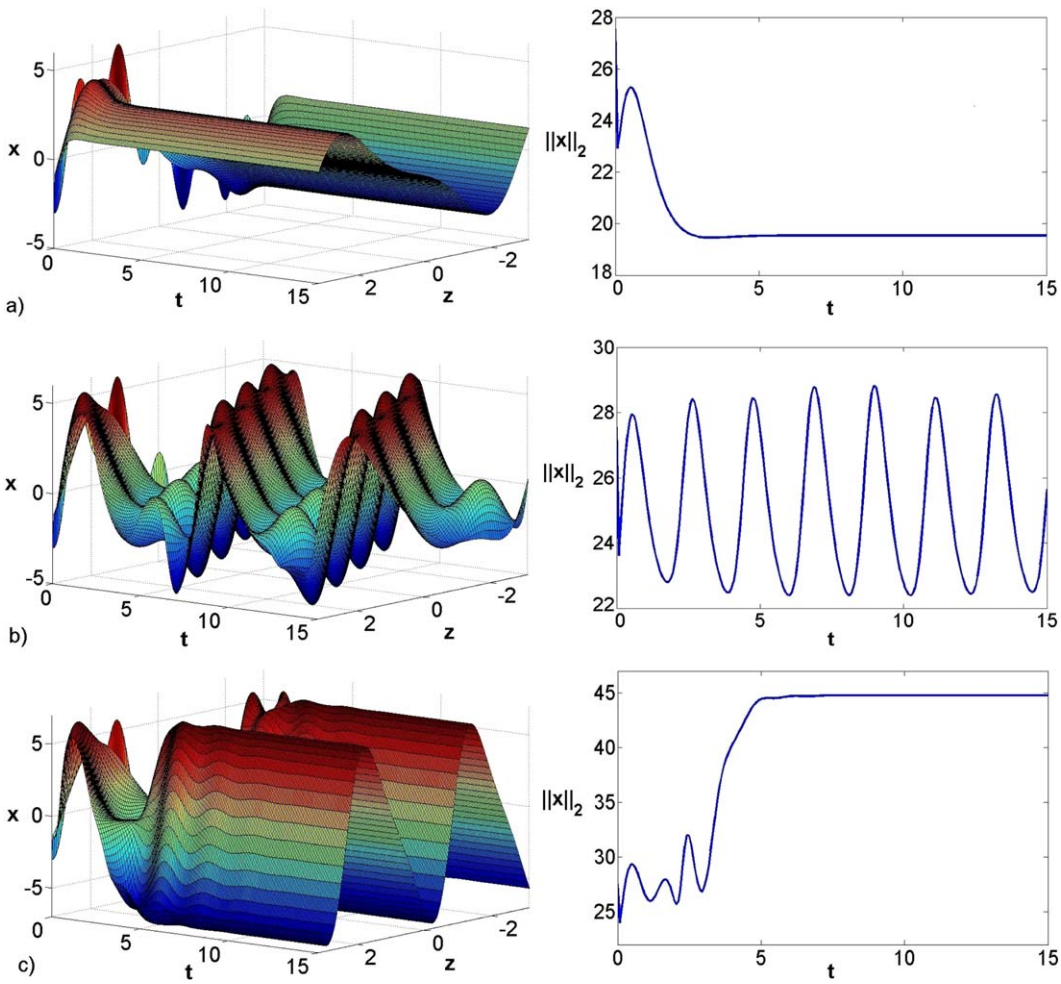

Figure 3. Open-loop spatiotemporal state profile (left) and norm of the state (right) for (a) $v=0.4$, (b) $v=0.23$, and (c) $v=0.15$.

[Color figure can be viewed in the online issue, which is available at wileyonlinelibrary.com.]

Supervisory Control

During system evolution, the ROM may need to be updated to remain accurate. The OLF, the CLF and finally the controller in (41) are redesigned based on the updated ROM using APOD when new snapshots arrive during the process evolution. Consequently, we need the stability tools of hybrid systems theory to prove that the closed-loop system remains stable during the periodic updates of the ROM. For this analysis, multiple Lyapunov functions (CLFs and OLFs) of the form (30) are considered. Under the assumption of finite time interval between ROM updates, the multiple Lyapunov functions of (30) for each ROM guarantee the Lyapunov stability of switching system (Theorem 3.2 in Ref. 32) when the following additional constrain is satisfied.

$$V_c(\hat{a}(t_k)) < V_c(\hat{a}(t_{k-1})), V_o(e(t_k)) < V_o(e(t_{k-1})) \tag{42}$$

where $k > 1$, $V_c(a(t_k))$ and $V_o(e(t_k))$ correspond to the value of Lyapunov function at the beginning of the interval k.

The Lyapunov functions may increase possibly during dimensionality changes of the ROM even when the offset is small. Thus, values of ζ_c and ζ_o need to be chosen appropriately using a supervisory control loop. We can then ascertain that for the chosen controller parameters the Lyapunov functions during controller redesign satisfy the conditions of switching systems stability theorem.[32,33] In general, higher values of ζ_c lead to more aggressive control action. A possible strategy is to automatically adjust ζ_c as follows

$$\zeta_{c,t_k} = \left(\frac{\varepsilon}{100}\right)\left(\frac{\hat{a}(t_{k-1})^T\hat{a}(t_{k-1})}{\hat{a}(t_k)^T\hat{a}(t_k)}\right) \tag{43}$$

in order to retain an aggressive controller throughout the process operation. The strategy used in the current work is to initialize ζ_c at value ζ_{in} and re-evaluate it only when V_c constraint in (42) is violated based on the formula of (43).[19] The specific strategy leads to less aggressive behavior while guaranteeing closed-loop stability of the system. A nonaggressive representation of (43) can be obtained as follows

$$\zeta_{c,t_k} = \min\left\{\zeta_{c,t_{k-1}}, \left(\frac{\varepsilon}{100}\right)\left(\frac{\hat{a}(t_{k-1})^T\hat{a}(t_{k-1})}{\hat{a}(t_k)^T\hat{a}(t_k)}\right)\right\} \tag{44}$$

The same strategy is also used for ζ_o because dynamic OLF, $V_o = \frac{\zeta_o}{2}e^T P_o e$, may also increase when the ROM dimensionality changes. The value of ζ_o needs be chosen appropriately to satisfy the conditions of switching systems stability theorem in Ref. 33 At the time, t_i, when the periodic snapshot measurements become available, the basis functions computed using APOD locally capture the subspace $\mathbb{H}_s$ and as a result we can directly compute the system state $\tilde{a}$ and the observer error, $e = \hat{a} - \tilde{a}$, at that instant from

$$x(z,t_i) = \sum_{k=1}^{m}\tilde{a}_k(t_i)\psi_k(z) \Rightarrow \tilde{a}_k(t_i) = \int_\Omega x(z,t_i)\psi_k(z)dz, k = 1,\ldots,m$$

where $x(z,t_i)$ is the snapshot of the system at switching time t_i. Thus, similar to the updating formula for ζ_c the following equation is used for updating ζ_o.

$$\zeta_{o,t_k} = \left(\frac{\varepsilon}{100}\right)\left(\frac{e(t_{k-1})^T e(t_{k-1})}{e(t_k)^T e(t_k)}\right) \tag{45}$$

For a less aggressive policy, similarly to ζ_{c,t_k}, that is, we may initialize ζ_o at value ζ_{in} and re-evaluate it based on the formula of (44) only when V_o constraint in (42) is violated. The nonaggressive representation of (45) can be obtained as follows

$$\zeta_{o,t_k} = \min\left\{\zeta_{o,t_{k-1}}, \left(\frac{\varepsilon}{100}\right)\left(\frac{e(t_{k-1})^T e(t_{k-1})}{e(t_k)^T e(t_k)}\right)\right\} \tag{46}$$

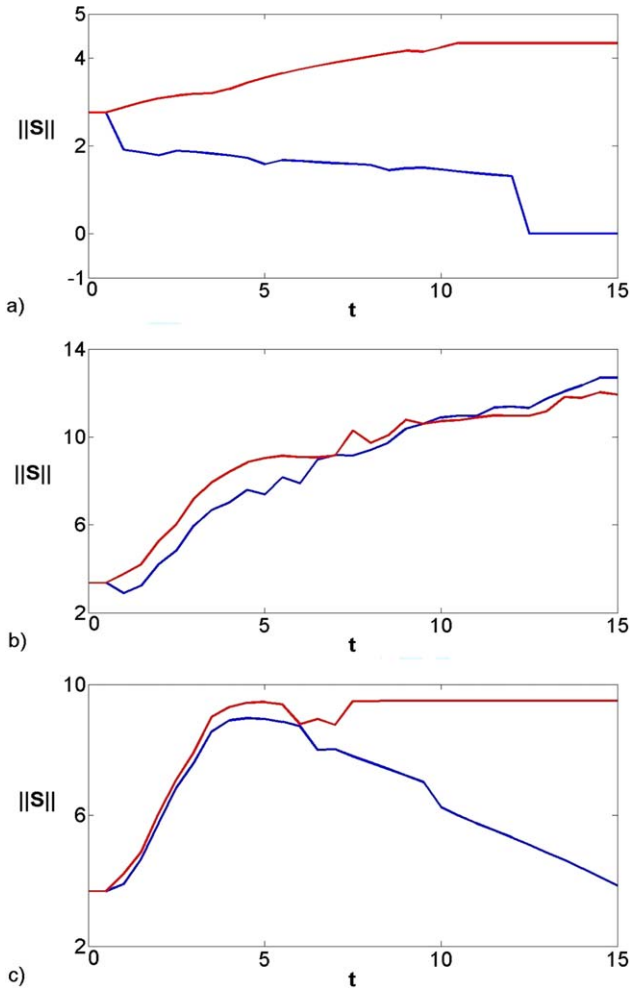

Figure 4. Open-loop temporal profile of norm of Shanon entropy using original APOD (blue lines) and modified APOD (red lines) for (a) $v = 0.4$, (b) $v = 0.23$, and (c) $v = 0.15$ (note the scale differences).

[Color figure can be viewed in the online issue, which is available at wileyonlinelibrary.com.]

Theorem 1. *Consider the nonlinear dissipative PDE system in (1) with Hilbert representation of (11) and its finite dimensional approximation of (13) with APOD obtained basis functions. We assume that*

- *the state modes of (1) can be partitioned into a finite number of slow and possibly unstable modes and an infinite number of stable and fast modes and there is a time scale separation between the dynamic behavior of the two subsystems,*
- *nonlinear function,* F, *in (13) is locally Lipschitz,*
- *locally,* $\mathbb{H}_s \subseteq \mathbb{P}$,
- *the time interval between ROM updates,* δt, *is finite and larger than a critical value,* t_b.

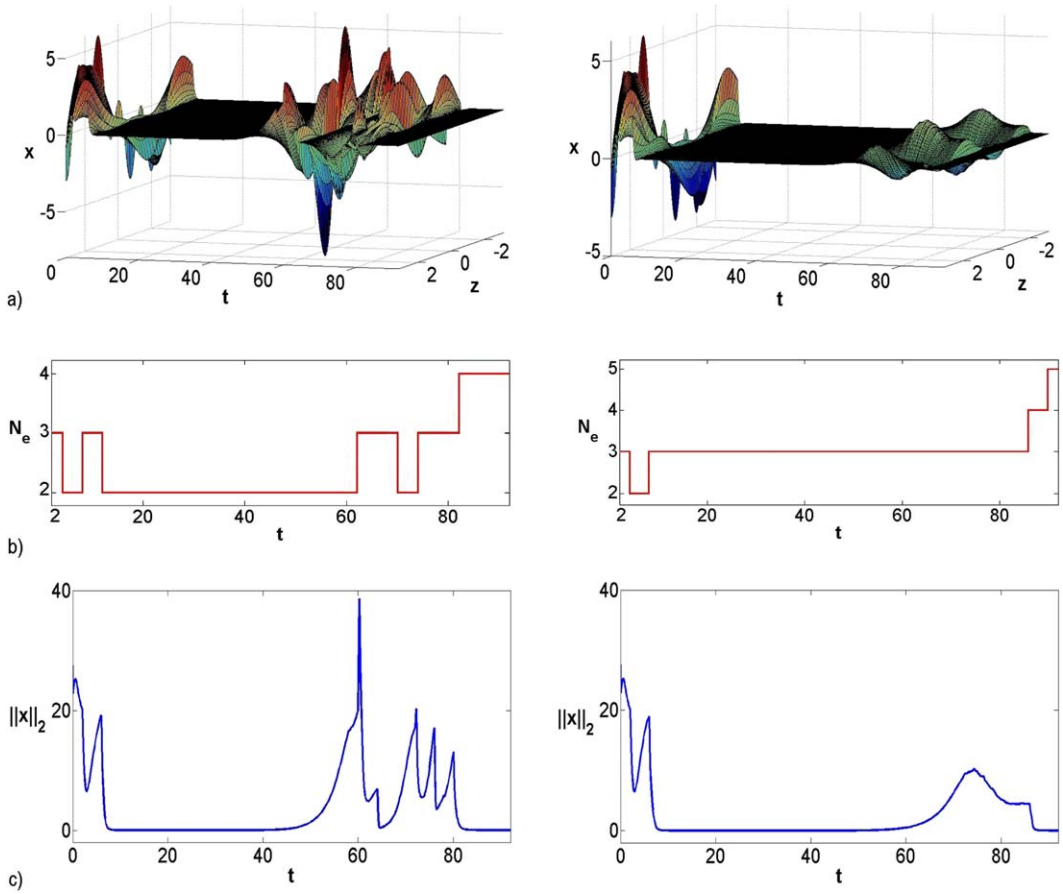

Figure 5. Closed-loop temporal profiles of (a) the state spatial profile (note the scale difference), (b) number of dominant eigenfunctions, and (c) norm of the state when v changes from 0.4 to 0.23 at $t = 40$.

The left figures present results when using original APOD and the right figures present results using modified APOD. [Color figure can be viewed in the online issue, which is available at wileyonlinelibrary.com.]

Under these assumptions, the system is locally asymptotically stable under the dynamic observer design of (27) with observer gain of (39) and the output feedback controller of (41) using supervisory control strategies of (43) and (45) for appropriately chosen control structure values, c_o, η, ξ, ε, and δt.

See Appendix C for proof.

Combining the model reduction procedure with the dynamic observer and controller synthesis methods, we have obtained an output feedback controller structure that guarantees that the closed-loop system evolves to the desired steady state. In Figure 2, the closed-loop process is presented under the proposed control structure in a block diagram form. The specific controller structure recursively redesigns the observer/controller components whenever the ROM is revised to retain relevancy and enforce closed-loop stability.

Remark 6. *Note that $\tilde{a}(t_k)$ is the initial condition for the dynamic observer at the beginning of the time interval k after updating procedure of ζ_c and ζ_o. This is possible because we obtain process snapshots, and thus state values of the dynamic observer are initiated to be the same as the state of the system.*

Remark 7. *In principle, the relaxation time periods t_b, in (64) can become arbitrarily small with the appropriate choice of slow subsystem dimensionality, s, due to the properties of dissipative systems. This directly translates into appropriately choosing parameter, ξ, in APOD.*

Application

Problem description

In this section, the ability of modified APOD in stabilizing the KSE is illustrated and compared to the original data ensembling approach in the absence and presence of uncertainty. KSE can adequately describe incipient instabilities arising in a variety of physico-chemical systems including falling liquid films, unstable flame fronts, interfacial instabilities between two viscous fluids.[34] The dynamic behavior of KSE with periodic boundary conditions has revealed the existence of steady and periodic wave solutions, as well as chaotic behavior.[35] Feedback control of KSE has been well studied in the literature.[18,36,37]

The integral form of the controlled KSE that is considered is

$$\frac{\partial x}{\partial t} = -v\frac{\partial^4 x}{\partial z^4} - \frac{\partial^2 x}{\partial z^2} - x\frac{\partial x}{\partial z} + \sum_{i=1}^{l} b_i u_i(t) \tag{47}$$

with periodic boundary conditions:

$$\frac{\partial^j x}{\partial z^j}(-\pi, t) = \frac{\partial^j x}{\partial z^j}(\pi, t), \qquad j = 0, \ldots, 3 \tag{48}$$

and initial condition

$$x(z, 0) = x_0(z) \tag{49}$$

where $x(z,t)$ is the system variable, $u(t) \in \mathbb{R}^l$ is the vector of control variables, t is the time, z is the spatial coordinate, $b(z)$

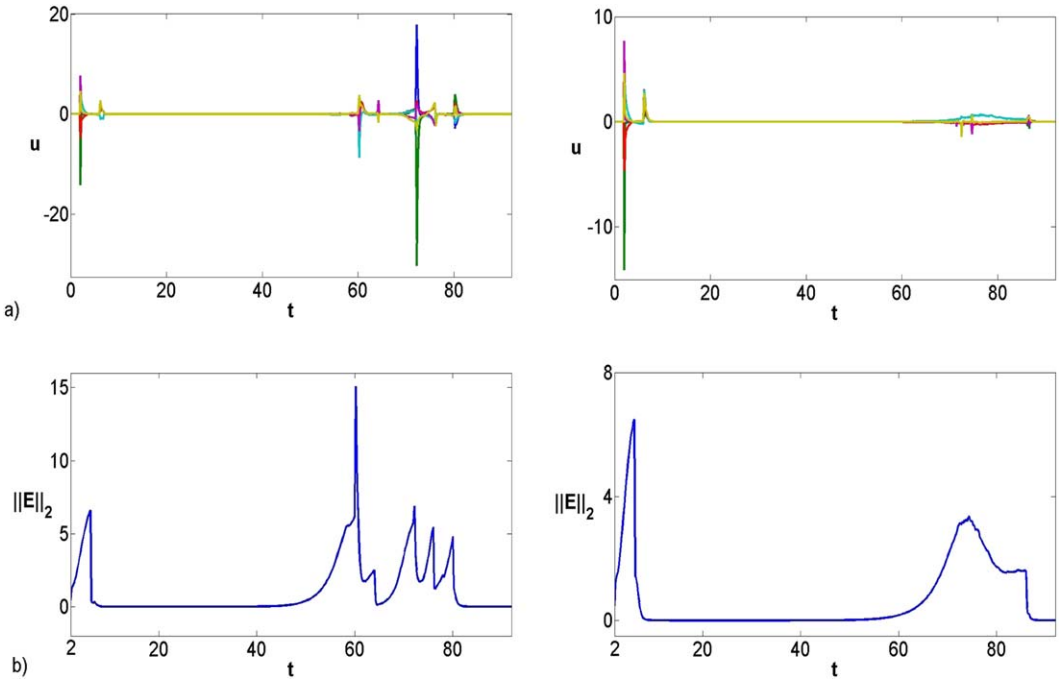

Figure 6. Closed-loop temporal profiles of (a) control action and (b) norm of error between the real system and the model when v changes from 0.4 to 0.23 at $t = 40$.

The left figures present results when using original APOD and the right figures present results using modified APOD (note the scale differences). [Color figure can be viewed in the online issue, which is available at wileyonlinelibrary.com.]

is a row vector describing the control actuators, and v is the diffusion parameter. Also in the above form $\mathcal{A}(z)=-v\frac{\partial^4}{\partial z^4}-\frac{\partial^2}{\partial z^2}$ and $\mathcal{F}(x)=-x\frac{\partial x}{\partial z}$. The Lipschitz condition for the nonlinear term in KSE, $\mathcal{F}(x)$, is discussed in Appendix D.

Six control actuators were assumed to be available at locations $L=[-\pi/2,-\pi/4,-\pi/6,\pi/5,\pi/4,\pi/2]$ and the corresponding spatial distribution functions at these locations are $b_i(z)=\delta(z-L_i)$ for $i=1,...,6$. The length of the spatial domain is 2π and continuous point measurement sensors placed uniformly across the domain of the process $(-\pi,\pi)$ are used. The continuous sensors shape distribution function, $s_m(z)$, for all time t, at these respective positions is $s_{m,i}(z)=\delta(z-z_i)$ for $i=1,...,5$, where z_i is the location of ith sensor unless otherwise stated. Also the periodic measurement sensor distribution function is assumed to be $s_r(z,t)=1$, that is, the complete profiles of the state as snapshots are available in specific time instants. Note that the specific actuators affect all the modes of the system. The following spatially nonuniform initial condition was considered $x_0=3\sin(z)-\cos(2z)-\sin(5z)+2\cos(5z)$. For both ensembling approaches,[31] snapshots of the process evolution we used. During the initial stage of populating the ensembles the snapshot interval was $\delta t=0.067s$. After that we assume the availability of snapshots of the process every $\delta t=2$ units of time during closed loop operation.

Comparison tools

In this section, we quantify the qualitative discussion in "the most important snapshots approach" section and compare the original and modified APOD.

Data sets often store redundant information. In other words, new entries may not convey independent information from other data in a set. In information theory and data mining communities, entropy is a measure of the information contained in a dataset; it quantifies the relative richness of data in the set. By extension there is a direct relationship between entropy and information contained in two similar sets with equal number of data.

A way to compare the efficiency of the original and modified APOD is through comparing their data ensembles. The ensemble entropy can provide an estimate of complexity of the spatial and temporal variations that illustrates which ensemble contains more independent profiles in their set.

Shanon entropy can be defined as[38]

$$S(z)=-\sum_{i=1}^{m}p_i(z)\ln\left(p_i(z)\right) \tag{50}$$

where m is the number of dominant eigenvalues and p_i is defined using the following equation

$$p_i(z)=\frac{\mu_i|\psi_i(z)|}{\sum_{j=1}^{m}\mu_j|\psi_j(z)|} \tag{51}$$

Note that the entropy is maximal and equal to 1 if the ensemble energy captured by the dominant eigenfunctions is distributed equally through all eigenfunctions and it is minimal and equal to 0 if only a single mode is captured. Larger entropy during system evolution indicates that the corresponding ensemble contains more information; thus, the corresponding ensembling approach is more efficient in retaining important information and can be used to construct ROMs with a wider range of accuracy.

Additionally, to provide a complete picture when comparing the performance of the two approaches, we define two performance indices: INC, the integral of norm of the control actions and INE, the integral of norm of the error between the real system and the model. The smaller values of INC and INE, the less control effort and more accurate model, respectively.

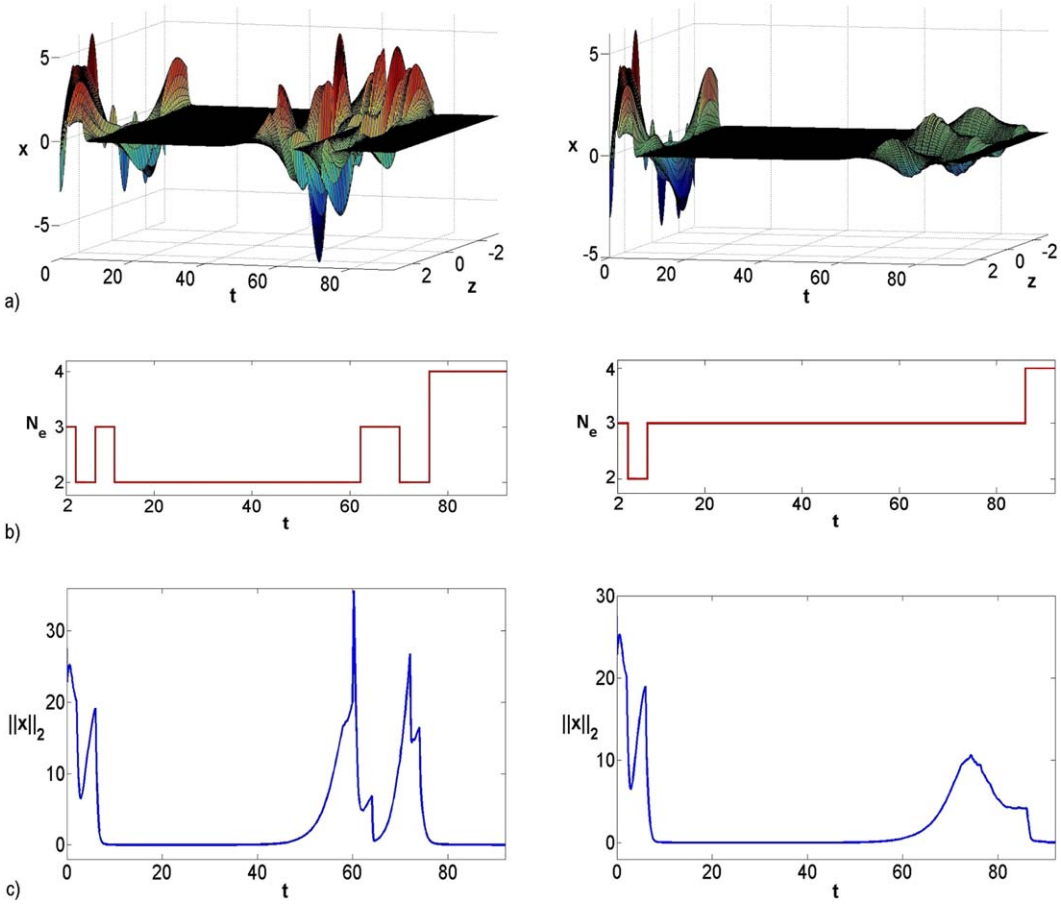

Figure 7. Closed-loop temporal profiles of (a) the state spatial profile, (b) number of dominant eigenfunctions, and (c) norm of the state in the presence of uncertainty when *v* changes from 0.4 to 0.23 at $t = 40$.

The left figures present results when using original APOD and the right figures present results using modified APOD (note the scale differences). [Color figure can be viewed in the online issue, which is available at wileyonlinelibrary.com.]

Simulation results

Figure 3 presents the open-loop profile and the spatial norm of the state of the KSE for v=0.4, 0.23 and 0.15, respectively. We observe that KSE exhibits complex behavior for $v < 1$ and the profile $x = 0$ is open-loop unstable. Thus, the control objective is to stabilize the system of (47)–(49) at the spatially uniform steady state $x_d(z,t)$=0. Figure 4 shows the temporal profile of norm of Shanon entropy when using the two APOD approaches to construct the ensembles. The blue and red lines present the norm of Shanon entropy using original and modified APOD, respectively. In Figures 4a, c, the Shanon entropy based on original APOD decreases during open-loop system evolution and converges to zero when the system reaches steady state while the entropy based on modified APOD increases or remains constant as old information is retained. In Figure 4b, the Shanon entropy based on both approaches increases due to oscillatory behavior of the open-loop system that causes continuous system excitation during process evolution. These results indicate that the ensemble based on modified APOD retains more information about the complex dynamics of KSE compared to the original one. As we will see later, this will result in a faster converging ROM to the true KSE dynamic behavior once we excite the system.

Focusing on the closed-loop system, during the initial time period t=[0, 2] of populating the ensembles, the process evolved with $u(t)$=0 (inactive controller). Application of off-line APOD to this ensemble resulted in 3 eigenfunctions for x which captured 99% of the energy embedded in the ensemble. As the availability of snapshots of the process is usually limited, we assume the availability of snapshots of the process every δt=2 units of time during closed loop operation. The following design parameter values were used to implement the control structure on the KSE: η=0.001, c_o=0.8, ζ_{in} =2, where ζ_{in} indicates the initial value for ζ_o and ζ_c.

Figure 5 presents the closed-loop process profile, number of dominant eigenfunctions and the norm of the state, respectively, for the original and the modified APOD when the diffusivity parameter, v, changes will be from 0.4 to 0.23 at $t = 40$ and the observer and controller know about the parameter change; this is called "the case without any uncertainty." We observe that for both approaches the controllers successfully stabilize the system of (47)–(49) at $x(z,t)$=0 while the state 2-norms converge smoothly to zero without any peaking. In both cases, the success of the designed controller in stabilizing the process at the desired profile is due to the dominant eigenspace (hence the ROM and the control law) being updated as the process traverses through different regions of the state space during closed-loop operation. The number of eigenfunctions required to capture the initial trends was three. During the closed-loop

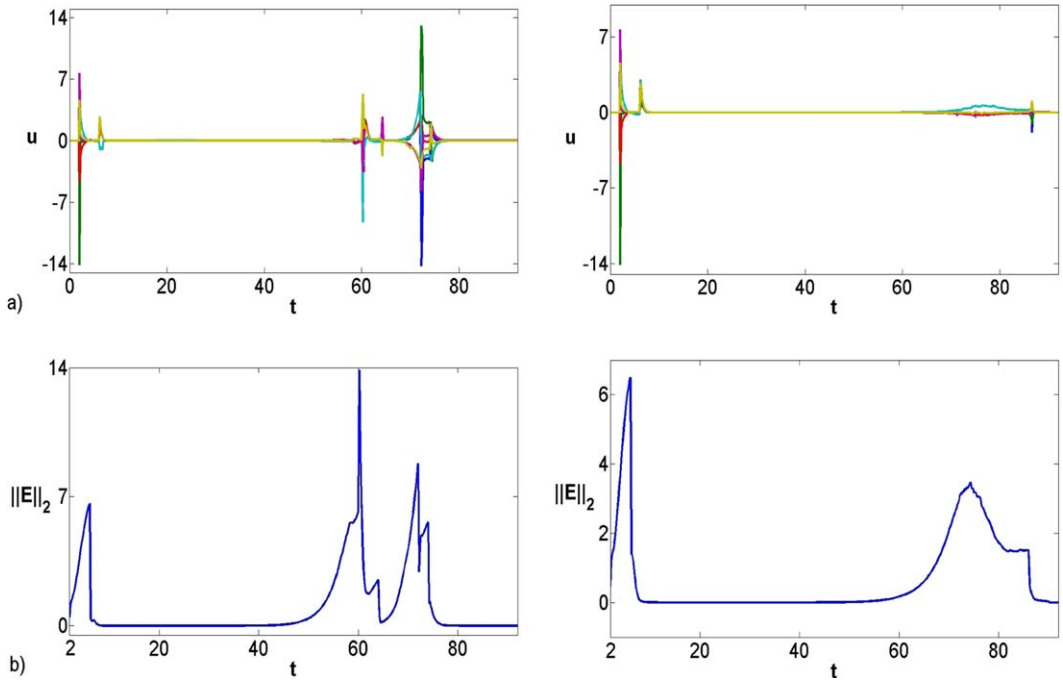

Figure 8. Closed-loop temporal profiles of (a) control action and (b) norm of error between the real system and the model in the presence of uncertainty when v changes from 0.4 to 0.23 at $t = 40$.

The left figures present results when using original APOD and the right figures present results using modified APOD (note the scale differences). [Color figure can be viewed in the online issue, which is available at wileyonlinelibrary.com.]

process operation, when new trends appeared the dominant eigenspace dimension was updated to accurately capture the process behavior, appropriately changing the number of empirical eigenfunctions. In general, the nonsmooth behavior of state 2-norm at specific times is due to fast modes' excitation and dimensionality changes. We observe that even though the change in v takes place at 40, it takes 10 sec for the new trends to become appreciable and another 5 sec for them to necessitate a ROM dimensionality change in order to capture all the unstable eigenmodes.

Figures 6a, b show the control actions and error norms between the real system and the ROMs, respectively. Using both approaches, the control actions and the model errors converge to zero and we do not observe any chattering when the parameter of the system changes and the controller/observer pairs is cognizant of this change. We observe a relatively large control action at the beginning of closed-loop region. It indicates that the controller tries to regulate the process using initially large control action. The error 2-norm converges to zero and there is a peaking at the beginning due to a peak in control action. Note that the nonsmooth behavior of control action and state 2-norm at specific times is also due to fast modes excitations caused by ROM revisions.

When v changes from 0.4 to 0.23 without any uncertainty the following indices show the improved performance of modified approach to the original approach in APOD; $INC_{or} = 93.02, INC_{\mathrm{mod}} = 34.01, INE_{\mathrm{or}} = 98.63, INE_{\mathrm{mod}} = 62.01$, where "or" and "mod" indicate the original and the modified ensembling approach in APOD. Based on the indices, we conclude modified APOD derived more accurate ROMs and constructed a" better" controller in this case, that required less control action to stabilize the system and responded better to the perturbation.

In the presence of uncertainty, the effectiveness of the modified approach becomes more apparent. Figure 7 shows the closed-loop process profile, number of dominant eigenfunctions and the norm of the state, respectively, for the original and the modified APOD when the diffusivity parameter, v, changes from 0.4 to 0.23 at $t = 40$ and the controller and the dynamic observer are not informed about the parameter change. We observe that the controllers still successfully stabilize the system of (47)–(49) at $x(z,t) = 0$ while the 2-norms converge smoothly to zero without any peaking. Figure 8 shows the control actions and the norms of error between the real system and the ROMs. Using both approaches, the control actions and the model errors converge to zero and we do not observer any chattering before

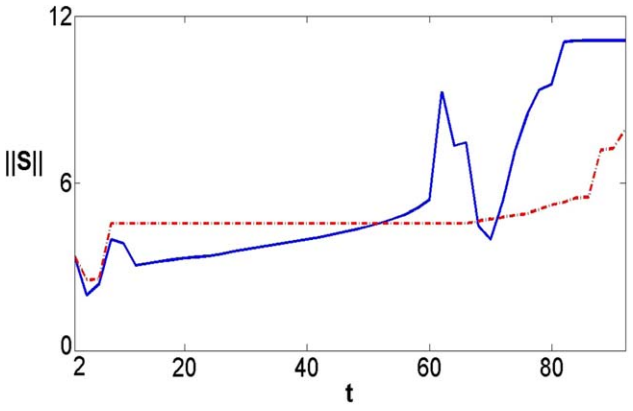

Figure 9. Closed-loop temporal profiles of Shanon entropy norm using original APOD (blue line) and modified APOD (red dashed line) in the presence of uncertainty, when v changes from 0.4 to 0.23 at $t = 40$.

[Color figure can be viewed in the online issue, which is available at wileyonlinelibrary.com.]

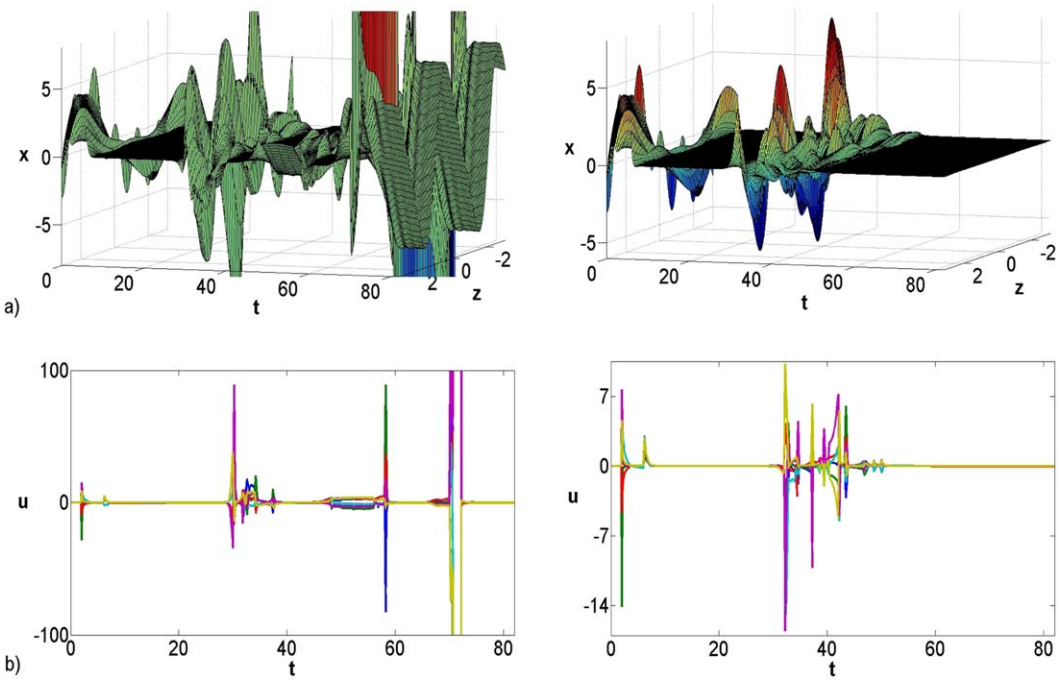

Figure 10. Closed-loop temporal profiles of (a) the state spatial profile and (b) control actions in the presence of uncertainty when v changes from 0.4 to 0.15 at $t = 25$.

The left figures present results when using original APOD and the right figures present results using modified APOD. [Color figure can be viewed in the online issue, which is available at wileyonlinelibrary.com.]

the parameter of the system changes. The following indexes indicate that the modified APOD has better performance compared to the original approach; $INC_{\text{or}} = 95.77, INC_{\text{mod}} = 32.66, INE_{\text{or}} = 90.73, INE_{\text{mod}} = 62.30$

Note that the control action using modified APOD is smoother than the control action using original APOD when the system changes in the absence and presence of uncertainty due to the faster ROM revisions in response to the changed system dynamics. Having less discontinuities in control action leads to less system excitation and reduces the observer/controller computation load. Large peaking or discontinuities in control action causes fast modes excitation. In

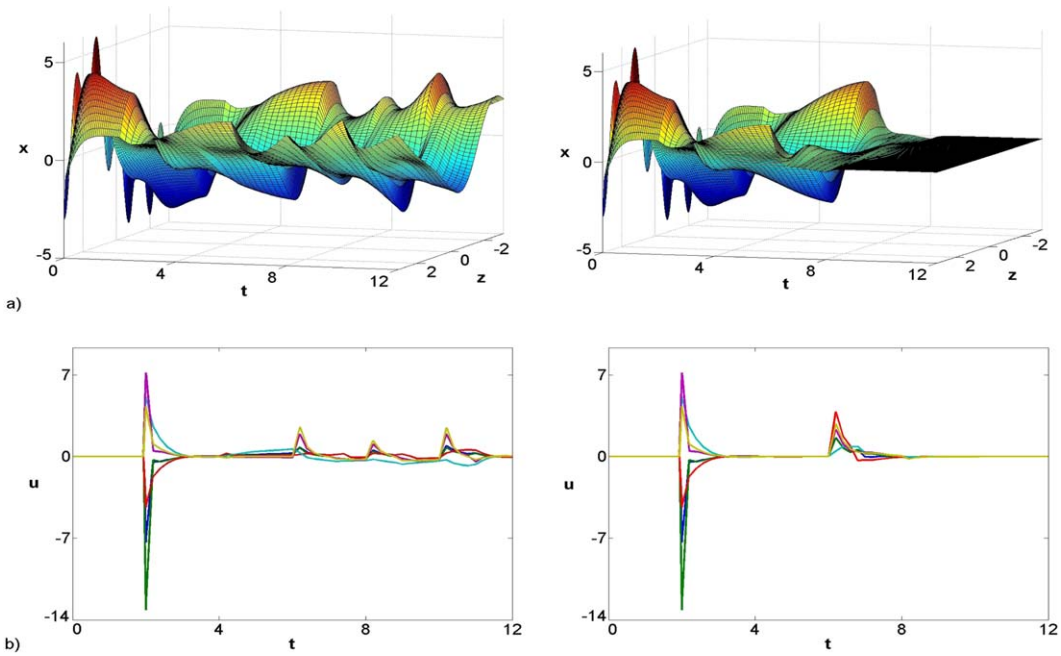

Figure 11. Closed-loop temporal profiles of (a) the state spatial profile and (b) control action using one point measurement sensor at $-\frac{\pi}{2}$.

The left figures present results when using original APOD and the right figures present results using modified APOD. [Color figure can be viewed in the online issue, which is available at wileyonlinelibrary.com.]

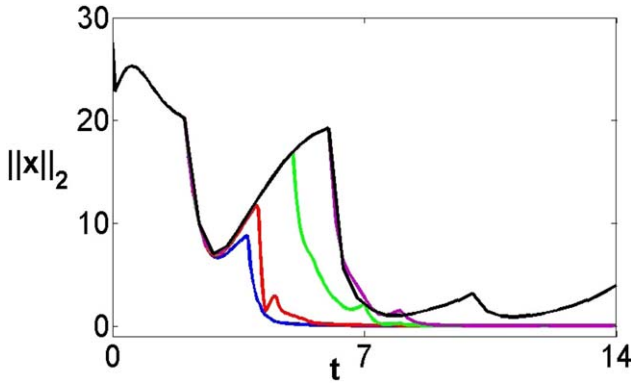

Figure 12. Closed-loop temporal profiles of norm of the state using one point measurement sensor at $-\frac{\pi}{2}$ for different availability of snapshots time periods, δt=0.25 (blue), δt=0.5 (red), δt=1 (green), δt=2 (pink), δt=4 (black), under modified APOD.

[Color figure can be viewed in the online issue, which is available at wileyonlinelibrary.com.]

response the basis functions change and the observer and controller need more revisions which increase the observer/controller computation load.

Figure 9 shows the temporal profile of the norm of Shanon entropy in the presence of uncertainty. It presents the information content measurement of the ensembles. During the time period before the change in the system parameter, the system entropy using modified APOD is more than the system entropy using original APOD that leads to construct more accurate ROM due to retaining the complex trends in the ensemble. When the system changes, the controller based on modified APOD adapted to the change rejection without any sharp control action due to more accurate ROM. However, the controller based on original APOD further excites the system with its sharp action and causes complex trends to resurface, which in turn increase the system entropy at time $t = 50$.

Figure 10 presents the case when the diffusivity parameter, v, changes from 0.4 to 0.15 at $t = 25$ unbeknownst to the control structure. The process dynamics then become very fast making the time interval between snapshots too large for standard APOD. The original APOD not only could not regulate the process but it further destabilized the system while the refined approach could still stabilize the closed-loop process at the desired steady state profile using reasonable control action. There is because the controllers based on modified APOD successfully stabilized the process as the ROM revisions were able to account for the changed dynamics faster.

In the APOD-based control of DPS using static observers that addressed in Refs. 17–19, the number of available point measurements should be equal to or greater than the dimension of ROM. One of the important advantages of using dynamic observers in this case is using less continuous point measurement sensors. Obviously, we want to use the minimum number of sensors to reduce costs even only one sensor when able to. The dynamic observer based on original APOD then becomes sensitive to the location and shape of the measurement sensor requiring sensor placement strategies. This limitation can be circumvented using modified APOD to construct observers that in general are more robust to the sensors locations and near unobservability, as it keeps information from previously traversed regions. Figure 11 presents the case when v=0.4 and only one point measurement sensor is used at $\frac{-\pi}{2}$. The original APOD could not regulate the process due to the unobservability while the refined approach still could stabilize the closed-loop process at the desired steady state profile using reasonable control action.

Figure 12 presents the closed-loop temporal profiles of norm of the state for different availability of snapshots time periods, δt when using one point measurement sensor at $-\frac{\pi}{2}$. It shows the relation between system dynamics and sampling time; when δt increases the fluctuations in 2-norm of the state will increase due to the states unobservability. In the first four cases when δt=0.25, δt=0.5, δt=1, and δt=2 the observer/controller can stabilize the system but in the final case, δt=4, the state 2-norm remains bounded but it does not converge to zero because the model uncertainty is larger than the threshold set during the initial controller design step.

Another important advantage of modified APOD is its robustness with respect to ensemble size to construct accurate ROMs. When using modified APOD a lower number of snapshots may be kept; this implies low dimensional covariance matrices will be derived that significantly improves the computational needs and memory requirements of the proposed controller/observer. This is illustrated in Figure 13 which presents the temporal profiles of the state and control action when v=0.4; only 11 snapshots are retained during the system evolution and only one sensor is used at $\frac{-\pi}{2}$, greatly reducing the computational load.

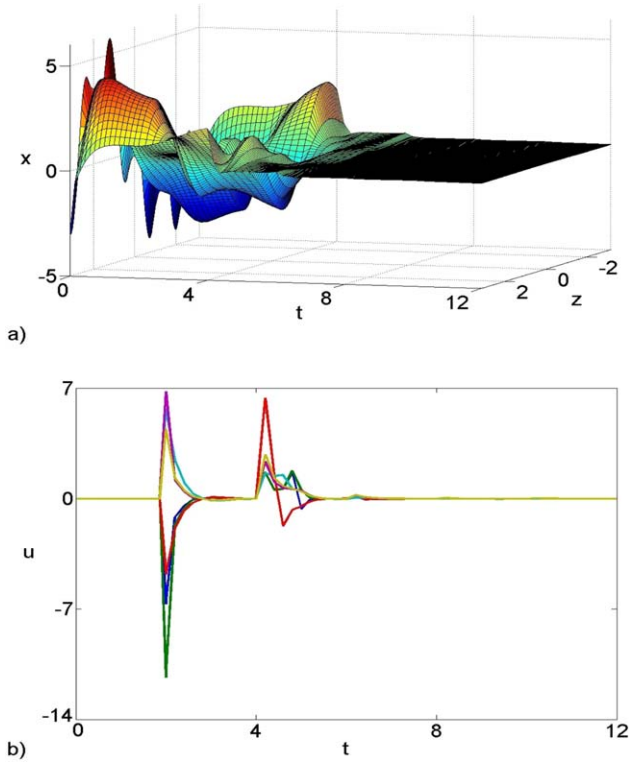

Figure 13. Closed-loop temporal profiles of (a) the state spatial profile and (b) control actions using an ensemble of 11 snapshots in modified APOD and a sensor at $-\frac{\pi}{2}$.

[Color figure can be viewed in the online issue, which is available at wileyonlinelibrary.com.]

Conclusions

In this article, the dynamic observer based control problem of DPS with limited state measurements was addressed by using a modified approach in APOD methodology. The stability of the closed-loop system was proven by Lyapunov stability criteria for hybrid systems. The proposed approach was successfully used to regulate the KSE at a spatially invariant steady state profile in the absence and presence of uncertainty when the open loop process exhibits highly nonlinear and chaotic behavior with fast transients.

Acknowledgment

Financial support from the National Science Foundation, CAREER Award # CBET 06–44519 is gratefully acknowledged.

Literature Cited

1. Armaou A, Christofides PD. Nonlinear feedback control of parabolic PDE systems with time-dependent spatial domains. *J Math Anal Appl*. 1999;239:124–157.
2. Christofides PD, Daoutidis P. Finite-dimensional control of parabolic PDE systems using approximate inertial manifolds. *J Math Anal Appl* 1997;216:398–420.
3. Garcia MR, Vilas C, Santos LO, Alonso AA. A robust multi-model predictive controller for distributed parameter systems. *J Process Control*. 2012;22:60–71.
4. Schuster E, Krstic M. Control of a non-linear PDE system arising from non-burning tokamak plasma transport dynamics. *Int J Control*. 2003;76:1116–1124.
5. Smyshlyaev A, Krstic M. On control design for PDEs with space-dependent diffusivity or time-dependent reactivity. *Automatica* 2005; 41:1601–1608.
6. Christofides PD. Nonlinear and Robust Control of PDE Systems. New York: Birkhäuser, 2000.
7. Sirovich L. Turbulence and the dynamics of coherent structures: Parts I, II and III. *Q Appl Math*. 1987;XLV:561–590.
8. Holmes P, Lumley JL, Berkooz G, Rowley CW. Turbulence, Coherent structures, Dynamical systems and Symmetry. New York: Cambridge University Press, 2012.
9. Alonso AA, Frouzakis CE, Kevrekidis IG. Optimal sensor placement for state reconstruction of distributed process systems. *AIChE J*. 2004;50(7):1438–1452.
10. Armaou A, Christofides PD. Finite-dimensional control of nonlinear parabolic PDE systems with time-dependent spatial domains using empirical eigenfunctions. *Int J Appl Math Comput Sci*. 2001;11:287–317.
11. Kunisch K, Volkwein S. Control of the Burgers equation by a reduced-order approach using proper orthogonal decomposition. *J Optim Theory Appl*. 1999;102:345–371.
12. Ly HV, Tran HT. Proper orthogonal decomposition for flow calculations and optimal control in a horizontal CVD reactor. *Q Appl Math*. 2002;60(4):631–656.
13. Ravindran SS. A reduced-order approach for optimal control of fluids using proper orthogonal decomposition. *Int J Numer Methods Fluids*. 2000;34(5):425–448.
14. Alsaggaf UM, Franklin GF. Model reduction via balanced realization: an extension and frequency weighted techniques. *IEEE Trans Automat Control*. 1988;33(7):687–692.
15. Ly HV, Tran HT. Truncated balanced realization of a stable nonminimal state-space system. *Int J Control*. 1987;46 (4):1319–1330.
16. Zhou K, Salomon G, Wu E. Balanced realization and model reduction for unstable systems. *Int J Robust Nonlinear Control*. 1999;9(3): 183–198.
17. Varshney A, Pitchaiah S, Armaou A. Feedback control of dissipative distributed parameter systems using adaptive model reduction. *AICHE J*. 2009;55:906–918.
18. Pitchaiah S, Armaou A. Output feedback control of distributed parameter systems using adaptive proper orthogonal decomposition. *Ind Eng Chem Res*. 2010;49:10496–10509.
19. Pitchaiah S, Armaou A. Output feedback control of dissipative PDE systems with partial sensor information based on adaptive model reduction. *AICHE J*. 2013;59(3):747–760.
20. Babaei Pourkargar D, Armaou A. Control of dissipative partial differential equation systems using APOD based dynamic observer designs. In: Proceeding of the American Control Conference. IEEE, Washington, DC, 2013:502–508.
21. Tarman IH, Sirovich L. Extensions to Karhunen-Loèvebased approximation of complicated phenomena. *Comput Methods Appl Mech Eng*. 1998;155:359–368.
22. Armaou A, Christofides PD. Dynamic optimization of dissipative PDE systems using nonlinear order reduction. *Chem Eng Sci*. 2002; 57:5083–5114.
23. Graham MD, Kevrekidis IG. Alternative approaches to the Karhunen-Loève decomposition for model reduction and data analysis. *Comput Chem. Eng*. 1996;20:495–506.
24. Temam R. Infinite-Dimensional Dynamical Systems in Mechanics and Physics. New York: Springer-Verlag, 1988.
25. Curtain RF, Zwart H. An Introduction to Infinite-Dimensional Linear Systems Theory. New York: Springer-Verlag, 1995.
26. Luenberger DG. Observing the state of a linear system. *IEEE Trans Milit Electron*. 1963;8:74–80.
27. Karafyllis I, Kravaris C. Robust output feedback stabilization and nonlinear observer design. *Sys Control Lett*. 2005;54:925–938.
28. Kazantzis N, Kravaris C. Nonlinear observer design using Lyapunov's auxiliary theorem. *Sys Control Lett*. 1998;34:241–247.
29. Soroush M. Nonlinear state-observer design with application to reactors. *Chem Eng Sci*. 1997;52:387–404.
30. Veillette RJ. Reliable linear-quadratic state feedback control. *Automatica* 1995;31:137–143.
31. Sontag E. A universal construction of artsteins theorem on nonlinear stabilization. *Sys Control Lett*. 1989;13:117–123.
32. Decarlo RA, Branicky MS, Pettersson S, Lennartson B. Perspectives and results on the stability and stabilizability of hybrid systems. *Proc IEEE*. 2000;88:1069–1082.
33. Christofides PD, El-Farra N. Control of Nonlinear and Hybrid Process Systems: Designs for Uncertainty, Constraints and Time-Delays. Berlin, Germany: Springer-Verlag, 2005.
34. Chang HC. Nonlinear waves on liquid film surfaces I. Flooding in vertical tube. *Chem Eng Sci*. 1986;41:2463–2476.
35. Kevrekidis IG, Nicolaenko B, Scovel JC. Back in the saddle again: a computer assisted study of the Kuramoto-Sivashinsky equation. *SIAM J Appl Math* 1990;50:760–790.
36. Armaou A, Christofides PD. Feedback control of the Kuramoto-Sivashinsky equation. *Phys D*. 2000;137:49–61.
37. Christofides PD, Armaou A. Global stabilization of the Kuramoto-Sivashinsky equation via distributed output feedback control. *Sys Control Lett*. 2000;39:283–294.
38. Bleris LG, Kothare MV. Low-order empirical modeling of distributed parameter systems using temporal and spatial eigenfunctions. *Comput Chem Eng*. 2005;29:817–827.
39. Khalil HK. Nonlinear systems. New Jersey: Prentice-Hall, 2002.

Appendix A: Proof of Proposition 1

Let $V_o = \frac{\zeta_o}{2} e^T e$ be the OLF for the dynamic observer system of (27); it can be shown that $e = 0$ is an equilibrium point for (29), $V_o(0) = 0$ and $V_o(e) > 0 \in \mathbb{R}^m - \{0\}$ where m is the number of the modes between ROM revisions. By substituting the observer gain that is computed from (39) in the system of (27) and assuming that the nonlinear function of f satisfies the Lipschitz condition, (32), it can be concluded that the OLF time derivative, $\dot{V}_o$, is negative definite and it only equals to zero at the equilibrium point. Thus based on Lyapunov's stability theorem (Theorem 4.1 in Ref. 39), there is δ_o such that when $||e(0)|| < \delta_o$ the observer error dynamics in (29) are locally asymptotically stable in the Lyapunov sense.

Appendix B: Proof of Proposition 2

Consider the system of (26) with candidate CLF defined as

$$V_c = \frac{\zeta_c}{2} \tilde{a}^T \tilde{a} \tag{52}$$

It is obvious that $V_c(0) = 0$ and $V_c(\tilde{a}) > 0 \in \mathbb{R}^s - \{0\}$ where s is the number of the modes of (26) between ROM

revisions. By substituting Eqs. 26 and 41 in the time derivative of the CLF, we obtain

$$\dot{V}_c = L_F V_c + L_B V_c u = -c_o(||L_B V_c||)^2 - \sqrt{(L_F V_c)^2 + (||(L_B V_c)||)^4} \tag{53}$$

Using appropriate values for the parameter c_o, it can be clearly observed that the time derivative of the CLF will be negative, $\dot{V}_c < 0$. Thus, based on Lyapunov's stability theorem (Theorem 4.1 in Ref. 39), there is a δ_c such that for $||\tilde{a}(0)|| < \delta_c$ the closed-loop system in (26) is locally asymptotically stable in the Lyapunov sense. Based on the designed fast stable observers and using the separation principle, the closed-loop process of (26) with the controller/observer pair will be asymptotically stable. Note that we use the observer state values, $\hat{a}$, for system states, $\tilde{a}$, in Eq. 41 based on the assumption of separation principle between dynamic observer and controller design.

Appendix C: Proof of Theorem 1

Part I. Closed-loop stability between ROM revisions

Substituting the controller (41) based on the states of (13) into the Hibert representation of the PDE system (11), we obtain

$$\begin{aligned} \dot{a}_s &= A_s(a_s, a_f) + F_s(a_s, a_f) - B_s k(\hat{a}, c_o)(L_B V_c) \\ \dot{a}_f &= A_f(a_s, a_f) + F_f(a_s, a_f) - B_f k(\hat{a}, c_o)(L_B V_c) \end{aligned} \tag{54}$$

where the initial conditions of the switching system in current time interval are the final states of the system in the previous time interval, and state estimate $\hat{a}$ is obtained from the dynamic observer of (27)

$$\dot{\hat{a}} = A\hat{a} + f(\hat{a}) + Bu + L(C\hat{a} - y_m) \tag{55}$$

where

$$y_m = S_m a_s + S_m a_f \tag{56}$$

Under the assumption of time scale separation of the PDE dynamics, the system of (54) can be expressed in the following singular perturbation form (sections 4.4 and 4.5 in Ref. 6) with dynamic observer of (55)

$$\begin{aligned} \dot{a}_s &= A_s(a_s, a_f) + F_s(a_s, a_f) - B_s k(\hat{a}, c_o)(L_B V_c) \\ \varepsilon_s \dot{a}_f &= \varepsilon_s A_f(a_s, a_f) + \varepsilon_s(F_f(a_s, a_f) - B_f k(\hat{a}, c_o)(L_B V_c)) \\ \dot{\hat{a}} &= A\hat{a} + f(\hat{a}) - Bk(\hat{a}, c_o)(L_B V_c) + L(C\hat{a} - S_m a_s - S_m a_f) \end{aligned} \tag{57}$$

where $\varepsilon_s = |\lambda_1|/|\lambda_{s+1}|$ is a small number that indicates the separation between the dominant and nondominant eigenmodes. In (57), $A_{f\varepsilon_s} = \varepsilon_s A_f$ has negative eigenvalues of $O(1)$ (due to the definition of A_f and ε_s) and $F_f(a_s, a_f) - B_f k(\hat{a}, c_o)(L_B V_c)$ does not contain terms of $O\left(\frac{1}{\varepsilon_s}\right)$ locally for the specific controller design.[2,6] By defining $\tau = t/\varepsilon_s$ and setting $\varepsilon_s = 0$, the fast subsystem dynamics of (57) can be expressed in the following fast time scale form

$$\frac{\partial a_f}{\partial \tau} = A_{f\varepsilon_s} a_f \tag{58}$$

The solution of the locally exponentially stable system of (58) then is

$$a_f(\tau) = a_f(0) e^{A_{f\varepsilon_s}\tau} \tag{59}$$

Focusing on the norm of a_f, from (59) and Schwartz inequality we obtain

$$||a_f(\tau)||_2 = ||a_f(0) e^{A_{f\varepsilon_s}\tau}||_2 \le ||a_f(0)||_2 ||e^{A_{f\varepsilon_s}\tau}||_2 \tag{60}$$

The definition of $A_{f\varepsilon_s}$ and the eigenspectrum bound to the fast subsystem imply that

$$||a_f(0)||_2 ||e^{A_{f\varepsilon_s}\tau}||_2 \le ||a_f(0)||_2 e^{(\varepsilon_s \lambda_{s+1})\tau} \tag{61}$$

where λ_{s+1} represents the dominant eigenvalue of A_f which is the least negative and of $O\left(\frac{1}{\varepsilon_s}\right)$. Using singular perturbation arguments for infinite dimensional systems it is shown that within a finite time the fast system dynamics will relax to a ball of radius $O(\varepsilon_s)$ around zero. Using the spectral bound of (60) and (61) for the dynamic behavior and that $\varepsilon_s = |\lambda_1|/|\lambda_{s+1}|$ we can obtain

$$||a_f(0)||_2 e^{(\varepsilon_s \lambda_{s+1})\tau} = ||a_f(0)||_2 e^{-|\lambda_1|\tau} \le O(\varepsilon_s) \tag{62}$$

it implies that

$$\tau_b = \frac{t_b}{\varepsilon_s} \ge -\frac{1}{|\lambda_1|} \ln\left[O\left(\frac{\varepsilon_s}{||a_f(0)||_2}\right)\right] \tag{63}$$

Thus,

$$t_b \ge \frac{1}{|\lambda_{s+1}|} \ln\left[O\left(\frac{||a_f(0)||_2}{|\lambda_1|}|\lambda_{s+1}|\right)\right] \tag{64}$$

Considering the time needed for relaxation of (57), t_b, and the time interval between ROM revisions, $\delta t = t_k - t_{k-1}$, we choose δt such that $\delta t > t_b$. For time, $t \ge t_b$ the closed-loop PDE system in (57) approximately reduces to the finite-dimensional slow system (Proposition 1 in Ref. 2),

$$\begin{aligned} \dot{a}_s &= A_s(a_s, 0) + F_s(a_s, 0) - B_s k(\hat{a}, c_o)(L_B V_c) \\ \dot{\hat{a}} &= A\hat{a} + f(\hat{a}) - Bk(\hat{a}, c_o)(L_B V_c) + L(C\hat{a} - S_m a_s) \end{aligned} \tag{65}$$

Based on Propositions 1 and 2, we obtain that the observation error Lyapunov function (OLF), V_o, and the output feedback CLF, V_c, are negative individually. Thus, the combined observer/controller structure can stabilize the states of (65) based on the assumption of separation principle between dynamic observer and controller design and considering (24) and (25). The time derivative of the Lyapunov function of the system, $\dot{V}$, is thus negative between ROM revisions

$$\dot{V} = \dot{V}_o + \dot{V}_c < 0 \tag{66}$$

Therefore, based on Lyapunov's stability theorem (Theorem 4.1 in Ref. 39), there is δ such that when $||a(0)|| < \delta$, the closed-loop system of (65) is locally asymptotically stable in the Lyapunov sense between ROM revisions. Thus, the nonlinear dissipative PDE system in (1) can be asymptotically stabilized by the dynamic observer design of (27) with observer gain of (39) and the output feedback controller in (41) between ROM revisions.

Part II. Closed-loop stability of the hybrid system

Considering ROM revisions, the closed-loop system behavior can be described by switched systems theory and the stability aspects of the closed-loop switched system need to be guaranteed using hybrid systems stability theorems. Based on the discussion in the "supervisory control" section

the obtained multiple observer and controller Lyapunov functions defined after each ROM revision need to satisfy the hybrid systems stability criteria. The supervisory control strategies in (43) and (45) directly enforce the Lyapunov stability of the switching systems criteria at the beginning of each time period, in the controller and observer designs (Theorem 3.2 in Ref. 32) and the CLF and OLF satisfy the conditions of (42) in the time intervals between switching. Thus, the closed-loop Lyapunov function satisfies the the Lyapunov stability of the switching systems,[32,33]

$$V(t_k)=V_c(\hat{a}(t_k))+V_o(\hat{a}(t_k)) < V_c(\hat{a}(t_{k-1}))+V_o(\hat{a}(t_{k-1})) \Rightarrow V(t_k) < V(t_{k-1})$$

It can be concluded that the designed observer of (35) and the output feedback controller in (41) pair using supervisory control strategies (43) and (45) asymptotically stabilize the switching close-loop system.

Appendix D: Lipschitz Condition for Nonlinear Term in KSE

The nonlinear term in KSE has a quadratic form of $\mathcal{F}(x)=-x\frac{\partial x}{\partial z}$. The important step in nonlinear analysis is finding a procedure to compute the Lipschitz parameter. We assumed that $||x(z,t)||_2 \le L_1(t)$, that is, the system state remained within a ball of radius $L_1(t)$ around the desired steady state and the spatial dynamics are bounded, that is, $||\frac{\partial x}{\partial z}(z,t)||_2 \le L_2(t)$ and $||\frac{\partial x_2}{\partial z}(z,t)-\frac{\partial x_1}{\partial z}(z,t)||_2 \le M(t)\ ||x_2(z,t)-x_1(z,t)||_2$. From the left-hand side of Lipschitz condition we obtain

$$||x_1\frac{\partial x_1}{\partial z}-x_2\frac{\partial x_2}{\partial z}||_2=||x_1\frac{\partial x_1}{\partial z}-x_2\frac{\partial x_1}{\partial z}+x_2\frac{\partial x_1}{\partial z}-x_2\frac{\partial x_2}{\partial z}||_2$$

$$\le ||x_2\frac{\partial x_1}{\partial z}-x_2\frac{\partial x_2}{\partial z}||_2+||x_1\frac{\partial x_1}{\partial z}-x_2\frac{\partial x_1}{\partial z}||_2$$

$$=||x_2||_2||\frac{\partial x_1}{\partial z}-\frac{\partial x_2}{\partial z}||_2+||\frac{\partial x_1}{\partial z}||_2||x_1-x_2||_2$$

thus

$$||x_1\frac{\partial x_1}{\partial z}-x_2\frac{\partial x_2}{\partial z}||_2 \le (L_1(t)M(t)+L_2(t))||x_1-x_2||_2$$

and the Lipschitz constant in the previous equation is $K_l(t)=L_1(t)M(t)+L_2(t)$.

Manuscript received Feb. 5, 2013, and revision received May 14, 2013.